In situ hydrostatic pressure induced improvement of critical current density and suppression of magnetic relaxation in Y(Dy$_{0.5}$)Ba$_2$Cu$_3$O$_{7-\delta}$ coated conductors

Lina Sang[1,2] , **Joffre Gutiérrez**[2], **Chuanbing Cai**[1,4], **Shixue Dou**[2] and **Xiaolin Wang**[2,3,4]

[1] Shanghai Key Laboratory of High Temperature Superconductors, Physics Department, Shanghai University, Shanghai 200444, People's Republic of China
[2] Institute for Superconducting and Electronic Materials, Faculty of Engineering, Australian Institute for Innovative Materials, University of Wollongong, NSW 2500, Australia
[3] ARC Centre of Excellence in Future Low-Energy Electronics Technologies, University of Wollongong, Australia

E-mail: cbcai@shu.edu.cn and xiaolin@uow.edu.cn

Abstract
We report on the effect of *in situ* hydrostatic pressure on the enhancement of the in-magnetic-field critical current density parallel to the crystallographic *c*-axis and vortex pinning in epitaxial Y(Dy$_{0.5}$)Ba$_2$Cu$_3$O$_{7-\delta}$ coated conductors prepared by metal organic deposition. Our results show that *in situ* hydrostatic pressure greatly enhances the critical current density at high fields and high temperatures. At 80 K and 5 T we observe a ten-fold increase in the critical current density under the pressure of 1.2 GPa, and the irreversibility line is shifted to higher fields without changing the critical temperature. The normalized magnetic relaxation rate shows that vortex creep rates are strongly suppressed due to applied pressure, and the pinning energy is significantly increased based on the collective creep theory. After releasing the pressure, we recover the original superconducting properties. Therefore, we speculate that the *in situ* hydrostatic pressure exerted on the coated conductor enhances the pinning of existing extended defects. This is totally different from what has been observed in REBa$_2$Cu$_3$O$_{7-\delta}$ melt-textured crystals, where the effect of pressure generates point-like defects.

Keywords: magnetic relaxation, critical current density, vortex pinning, metal organic deposition

(Some figures may appear in colour only in the online journal)

Introduction

Small magnetic relaxation and high critical current density (J_c) are crucial for technological applications of high temperature superconductors. So far, improved J_c has been reported by the pinning of vortices via local structural inhomogeneities in superconductors, which are induced by chemical doping [1], irradiation [2, 3], inclusion of non-superconducting secondary phases [4–6], or *in situ* hydrostatic pressure [7, 8]. The increase in J_c due to pressure has been typically attributed to the generation of point-like defects, introducing more pinning centers [9–11]. Additionally, it has been reported for different superconducting systems that hydrostatic pressure may have other effects, such as increasing the critical temperature (T_c) [12–15]; shrinking the unit cells and reducing the lattice parameters, leading to the reduction of anisotropy [14, 16]; and improving grain connectivity, overcoming the grain boundary weak-link problem

[4] Authors to whom any correspondence should be addressed.

[7, 17, 18]. Although vortex pinning enhanced by pressure is not technologically viable so far, the study of its effects has shed light on the origins of superconductivity and on how to improve the superconducting parameters. Previous studies on $YBa_2Cu_3O_{7-\delta}$ thin films [19], and $YBa_2Cu_4O_8$ and $Tl_2CaBa_2Cu_2O_8$ ceramics [20] have shown that the J_c increases with pressure due to two effects: (1) under hydrostatic pressure, the vacant oxygen sites in the grain boundary (GB) region are filled with additional oxygen anions, increasing the hole carrier concentration in the GB region. (2) A large intrinsic increase in J_c occurs due to chemical compression of the GB itself [17, 18, 21, 22].

Most technological applications of high temperature superconductors, however, do not involve polycrystalline crystals or films, but rather so-called coated conductors, which are films epitaxially grown on long-length highly-textured buffered metallic tapes [4, 23]. State-of-the-art coated conductors have the highest critical current densities among superconducting materials and have been incorporated in a variety of in-magnetic-field applications, such as wires for electrical transport, magnets, fault current limiters, transformers, motors, generators, and flywheels [24]. Nevertheless, little is known about the effects of *in situ* hydrostatic pressure on these systems.

In this paper, we introduce the first systematic study of *in situ* hydrostatic pressure induced improvement of critical current density and vortex pinning in state-of-the-art $Y(Dy_{0.5})Ba_2Cu_3O_{7-\delta}$ coated conductors. In addition, the vortex dynamics are investigated through magnetic relaxation studies at different temperatures, fields, and pressures.

Experimental details

The coated conductors we have studied consist of $Y(Dy_{0.5})Ba_2Cu_3O_{7-\delta}$ films 1.0 μm thick that were epitaxially grown on top of highly-textured buffered Hastelloy substrates. The $Y(Dy_{0.5})Ba_2Cu_3O_{7-\delta}$ layer was fabricated by metal organic deposition (MOD). The studied samples were laser-cut from large-sized $Y(Dy_{0.5})Ba_2Cu_3O_{7-\delta}$ coated conductors into a square geometry of 1.1×1.1 mm^2. A set of 30 samples were neatly stacked together into a high pressure tube. An HMD high pressure cell and Daphne 7373 oil were used as the medium to impose *in situ* hydrostatic pressure on the samples. Further details on the experimental set up can be found in the Quantum Design High Pressure Cell User Manual. Magnetic measurements at different temperatures were performed by using a quantum design physical properties measurement system equipped with a vibrating sample magnetometer.

Field-cooled (FC) measurements were performed after applying a magnetic field of 10 Oe above T_c. Zero-field-cooled (ZFC) measurements were performed by cooling down the samples below T_c in the absence of a magnetic field and then applying 10 Oe. In both cases the magnetic moment was measured while ramping up the temperature. The values of the critical current density were obtained by applying the Bean critical state model on magnetization hysteresis loops of fully penetrated samples. Similarly, for magnetic relaxation measurements, the sample was in the fully penetrated critical state, and the applied magnetic field was increased from -8 T up to the field at which the magnetic relaxation was measured. The time dependence of the magnetization $M(t)$ was recorded for 1 h.

Results and discussion

The inset to figure 1(a) shows the resistivity as a function of temperature at zero magnetic field and *in situ* hydrostatic pressure. A sharp transition from the superconducting to the normal state is observed, with T_c at the mid-point of the transition located at 93.8 K, with the width of the transition, $\Delta T_c = 0.4$ K. Figure 1(a) shows the temperature dependence of the magnetic moment for ZFC and FC measurements at *in situ* hydrostatic pressure, HP = 0 and HP = 1.2 GPa. No detectable change in T_c is observed under the highest pressure we can reach in the ZFC magnetization curves. Note that similar results were previously reported for $Ba_{0.6}K_{0.4}Fe_2As_2$ thin films [25]. The J_c is calculated from the $M–H$ loops (as presented in figure 1(b)) using the Bean model [26], $J_c = 20 \Delta M/Va(1 - a/3b)$, where ΔM is the loop width, V is the sample volume, and a and b are the sample dimensions perpendicular to the field direction, $a < b$. The self-field J_c is remarkably high, 1.5×10^7 and 2×10^6 A cm^{-2} at 2 and 77 K, respectively, confirming the high quality of the samples. At temperatures close to T_c and at high fields, the magnetic signal of the Hastelloy substrate becomes comparable to that of the superconductor. In order to subtract the signal from the metallic substrate, we measured substrates (with the same geometry as the samples) under the same conditions as for the superconducting samples (inset to figure 1(b)). Figure 1(c) shows the field dependence of J_c at 2 K, 40 K, 70 K, and 77 K, with and without pressure, respectively. Within the temperature range from 2 to 40 K J_c shows almost no relative change under pressure. On the contrary, at higher temperatures the *in situ* hydrostatic pressure significantly enhances J_c above a certain crossover magnetic field that we have denoted as H_{PE}. We quantify H_{PE} as the magnetic field for which the ratio of $(J_c(1.2\ \text{GPa}) - J_c(0\ \text{GPa}))/J_c(0\ \text{GPa}) > 0.1$. As we come close to the irreversibility line, the enhancement in J_c is more dramatic. As shown in figure 1(d), at 77 K and 5 T, J_c is enhanced by more than a factor of five under 1.2 GPa (from 2×10^3 A cm^{-2} at 0 GPa to 1.1×10^4 A cm^{-2} at 1.2 GPa), achieving a factor of ten increase at 80 K and 5 T for 1.2 GPa.

Figure 2 shows both H_{PE} and the irreversibility line as functions of temperature. The irreversibility line (H_{irr}) is deduced from J_c versus B, using the criterion of $J_c = 1 \times 10^3$ A cm^{-2}. Under *in situ* hydrostatic pressure, the irreversibility line is shifted to higher fields (without changing T_c, as shown in figure 1(a)).

It is important to highlight that these findings are very different from previous pressure studies on melt-textured $YBa_2Cu_3O_{7-\delta}$ bicrystalline rings containing single [001]-tilted GBs [17, 18]. In melt-textured $YBa_2Cu_3O_{7-\delta}$ it was
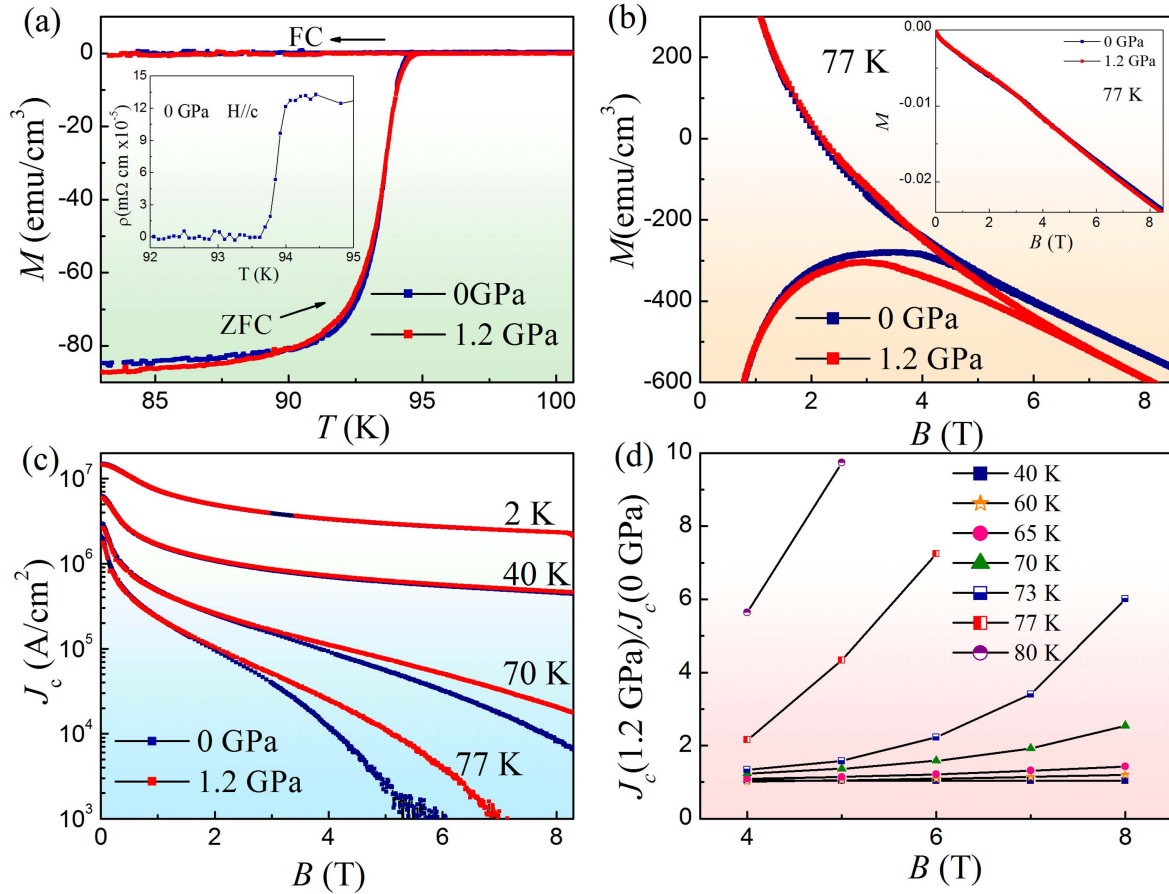
Figure 1. (a) The magnetic moment temperature dependence under ZFC and FC conditions shows no dependence on the applied *in situ* hydrostatic pressure ($P = 0$ and $P = 1.2$ GPa) for Y(Dy$_{0.5}$)Ba$_2$Cu$_3$O$_{7-\delta}$ coated conductors. Inset: the resistivity versus temperature at zero field shows a sharp superconducting to normal state transition at 93.8 K. (b) The magnetic moment versus applied magnetic field loops are used in combination with the Bean critical state model to obtain the J_c values. At high temperatures and fields, the signal from the substrate significantly alters the superconducting signal. Inset: magnetic moment versus applied magnetic field of the metallic substrate. (c) J_c versus applied magnetic field at 2, 40, 70, and 77 K under $P = 0$ and 1.2 GPa. The effect of the *in situ* hydrostatic pressure on J_c is only noticeable at high temperatures and fields. (d) The ratio $J_c(1.2\ \text{GPa})/J_c(0\ \text{GPa})$ as a function of the magnetic field for different temperatures shows that the effect of pressure on J_c becomes higher as the temperature and magnetic field increases.

shown that a strong increase in J_c at low temperatures and fields occurred under the effect of *in situ* hydrostatic pressure. The effect was attributed to the increase of the hole carrier concentration in the GB region. The melt-textured YBa$_2$Cu$_3$O$_{7-\delta}$ bicrystalline ring samples contained large angle GB (LAGB) misorientations ($>10°$), while coated conductors have small angle GB (SAGB) misorientations ($<5°$). It has been calculated that, for a LAGB, the vortex structure at the GB deviates from the typical Abrikosov vortex, which becomes a mixture of a Josephson and an Abrikosov vortex [27]. Those Abrikosov–Josephson vortices are more difficult to pin by defects due to their deformed core. On the other hand, at a SAGB the vortex fully retains its Abrikosov structure and is efficiently pinned by the defects at the GB [28]. Contrary to what was found in the melt-textured samples, our results show a strong increase in J_c at high temperature and high fields, and a shift of the H_{irr} towards higher fields. This cannot be explained by an increase of hole carrier concentration in the GB region, and it is a typical signature of the proliferation of extended defects. Nevertheless, our experiments show that once the pressure

is released, both J_c and H_{irr} recover their initial values for $P = 0$ GPa. These results suggest that applying hydrostatic pressure up to 1.2 GPa does not generate new defects in the film microstructure. Therefore, we speculate that the *in situ* hydrostatic pressure enhances the strain fields around existing defects, such as twin boundaries, nanoparticles (size 10–100 nm) of rare-earth oxides (RE$_2$O$_3$) [29] and SAGBs [30] increasing the pinning force on the Abrikosov vortices at the GB. We will discuss this further when analyzing the magnetic relaxation data.

Now we discuss in more depth the possible flux pinning mechanisms for the pressure induced enhancement of J_c in the samples. Figure 3 shows the normalized pinning force as a function of h^* at different temperatures and for two hydrostatic pressures, 0 GPa and 1.2 GPa, where $h^* = H/H_{max}$ and H_{max} is the magnetic field where the flux pinning force density, F_p, reaches its maximum. According to the Dew-Hughes model $f_p \propto h^p(1 - h)^q$, where $h = H/H_{irr}$, different p and q fitting parameters can define the specific pinning mechanism. In this classical model, vortex pinning arising from different defects with different geometries and pinning strengths give rise to a
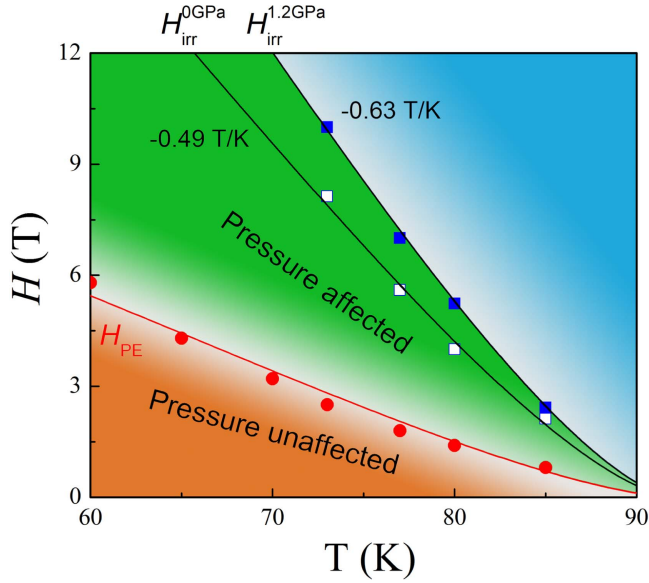
Figure 2. *H−T* diagram showing the region where the *in situ* hydrostatic pressure enhances superconductivity, both J_c and shifting the vortex liquid phase (H_{irr}) to higher temperatures and fields.
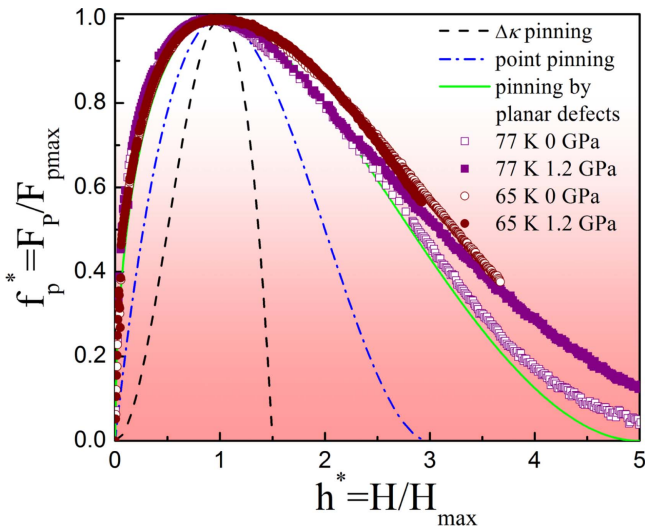

Figure 3. Normalized pinning force as a function of the normalized magnetic field, showing that the main source of pinning remains unchanged under the effects of pressure and that the pinning is due to planar defects.

different set of *p* and *q* parameters. The exponents $p = 1$ and $q = 2$ represent point pinning, defective regions whose dimensions in all directions are less than the inter-vortex spacing $d = 1.07(\phi_0/B)^{1/2}$; $p = 1/2$ and $q = 2$ describes pinning by planar defects such as GBs, twin boundaries, stacking faults and plate-like precipitates; and $p = 2$ and $q = 1$ represents pinning due to small differences in the Ginzburg number κ arising from changes in the normal state resistivity (referred to as $\Delta\kappa$ pinning). Due to it is difficult to determine H_{irr}, the scaling of the $f^*(h^*)$ data can be given by the following equations, $f^*(h^*) = (9/4)h^*(1 - h^*/3)^2$ for point pinning, $f^*(h^*) = (25/16)h^{*1/2}(1 - h^*/5)^2$ for pinning from planar

defects and $f^*(h^*) = 3h^{*2}(1 - 2h^*/3)$ for $\Delta\kappa$ pinning [31–33]. Figure 3 shows that all the curves collapse into a single master curve. Therefore, we may conclude that the main source of pinning, although enhanced, does not change due to the increase of pressure up to 1.2 GPa. It is also clearly shown according to the Dew-Hughes model (solid lines in figure 3) that the main source of vortex pinning is most probably due to the strain fields of planar-like defects. Due to the nature of the MOD coated conductors these planar defects are likely twin boundaries, nanodots (size 10–100 nm) of rare-earth oxides (RE$_2$O$_3$) and SAGBs [29].

To further elucidate on the effects of *in situ* hydrostatic pressure on the vortex pinning and dynamics in Y(Dy$_{0.5}$)Ba$_2$Cu$_3$O$_{7-\delta}$ coated conductors, we measured the time (*t*) dependence of the magnetization within the temperature and magnetic field ranges between 2–77 K and 1–7 T respectively using SQUID magnetometry. Figure 4(a) shows the normalized relaxation rate $S = |d\ln(J)/d\ln(t)|$ as a function of temperature at 1 and 3 T with and without pressure. At lower temperatures (<60 K) and fields ($H = 1$ T), S shows the usual small temperature dependence region with the relatively high vortex creep rate of cuprate superconductors [34]. This behavior arises from the glassy vortex dynamics that is characteristic of collective creep from random disorder [35]. As the field is increased (i.e. $H = 3$ T) and extended defects become more efficient as pinning centers as compared to random disorder, S increases linearly with temperature. In the *H–T* region covered in figure 4(a), S is not very affected by the *in situ* hydrostatic pressure. Nevertheless, it is worth noting that at 40 K and 3 T and at 40 K and 5 T [figure 4(b)] we are already able to observe a suppression of the relaxation rate due to the effect of 1.2 GPa of *in situ* hydrostatic pressure. As we show in figure 1(c), under the very same conditions, the critical current density is not affected.

This hints that we are not generating extra extended defects along the *c*-axis as we might suspect from the J_c data, as correlated defects along the *c*-axis tend to increase S instead of reducing it [36]. It is thus most probable that the hydrostatic pressure increases the strain fields around existing planar-like defects. It has been reported before that strain fields are very effective pinning centers [37, 38]. At high temperature and high magnetic fields, the relaxation rate S is significantly suppressed with 1.2 GPa of pressure. In this region of the *H–T* diagram, the same defects induced by hydrostatic pressure that enhance the J_c are responsible for the strong suppression of S.

According to the collective-pinning theory [35], the magnetic relaxation rate S can be written as

$$S = \frac{T}{U_0 + \mu T \ln(t/t_{eff})}.$$

Where t_{eff} is the effective hopping attempt time, U_0 is the flux activation energy in the absence of flux creep, and μ is a glassy exponent that contains information about the size of the vortex bundle in the collective creep theory [39]. At high enough temperatures ($U_0 \ll T$) the second term in the denominator
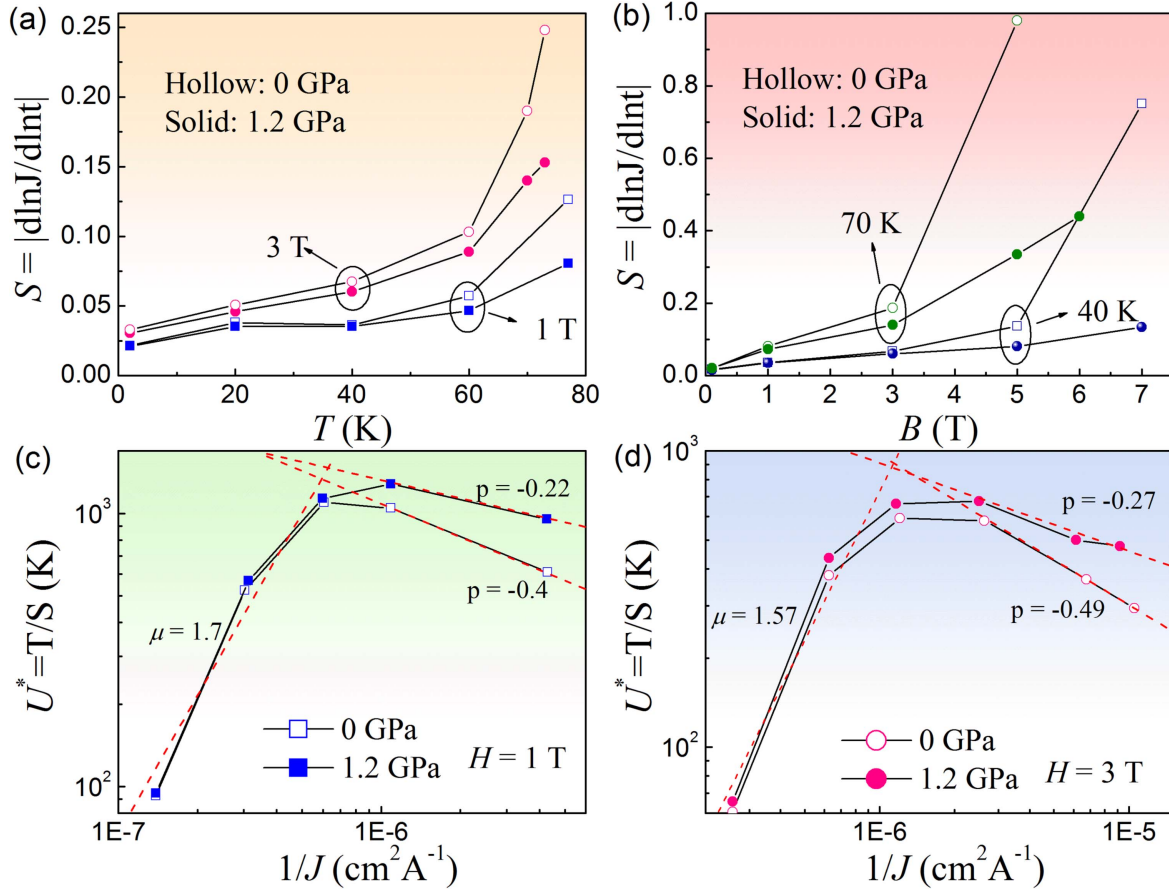
Figure 4. The temperature dependence (a) and the magnetic field dependence (b) of the magnetic relaxation rate S are decreased under the effect of *in situ* hydrostatic pressure. Dependence of the effective pinning energy U^* on inverse current density at 1 T (c) and 3 T (d) under $P = 0$ and $P = 1.2$ GPa for $Y(Dy_{0.5})Ba_2Cu_3O_{7-\delta}$ coated conductors.

dominates and we can approximate $S \sim 1/\mu \ln(t/t_{eff})$, predicting that S will have a plateau, as is observed experimentally.

According to the collective-pinning theory, the effective pinning barrier $U^*(J)$ $(= T/S)$ follows a nonlinear dependence on the inverse current density of the form $(1/J)^\mu$ [35, 39], with μ being the aforementioned glassy exponent. In a three-dimensional system, for vortex hopping lengths shorter than the Abrikosov lattice parameter, it is predicted that $\mu = 1/7$ in the low-field, low temperature region where the creep is controlled by the hopping of a single vortex; $\mu = 3/2$ for the collective creep of small bundles; and $\mu = 7/9$ for the large-bundle regimes, where the bundle size is much larger than the London penetration length [35]. In the opposite case, where the vortex hopping distance is larger than the Abrikosov lattice parameter, it is predicted that $\mu = 1/2$ [35]. In figures 4(c) and (d) we show U^* as a function of $1/J$ at 1 and 3 T with and without *in situ* hydrostatic pressure. $U^*(J)$ shows a non-monotonic dependence. At high J, the glassy exponent μ is positive and shows no change under 1.2 GPa. The values of μ are 1.7 and 1.57 at 1 and 3 T respectively, close to what was reported for (Gd–Y)–Ba–Cu–O films [40], and close to the value of 3/2, suggesting that the dissipation arises from the elastic creep of small bundles. After the maximum of $U^*(J)$, μ becomes negative, which is attributed to the faster escape of vortices from the superconductor in plastic creep

theory. Contrary to the above of $\mu > 0$, the negative slope is often denoted as p in plastic creep theory [41, 42]. Without pressure, we obtain values of μ close to 1/2, suggesting that the hopping distance of vortices in this region (at high temperatures) is larger than the Abrikosov lattice parameter [41]. In this high temperature region, we observe how the *in situ* hydrostatic pressure increases the glassy exponent (less negative), suggesting a change in the dissipation mechanism triggered by the effects of *in situ* hydrostatic pressure.

Conclusions

We have studied the critical current density and vortex pinning of epitaxial $Y(Dy_{0.5})Ba_2Cu_3O_{7-\delta}$ coated conductors prepared by metal organic deposition under *in situ* hydrostatic pressure. It is revealed that *in situ* hydrostatic pressure enhances the irreversibility line while it leaves T_c unchanged. J_c increases rapidly under pressure at high fields and temperatures, with the ratio of $J_c(1.2$ GPa)/$J_c(0$ GPa) reaching values of 10 close to the irreversibility line. The study of vortex dynamics through magnetic relaxation at various temperatures and fields reveals that the effect of pressure is most likely that of enhancing the strain fields at existing

planar-like defects, rather than generating new defects in the sample. Under pressure, vortex creep rates are significantly suppressed at high temperatures and fields and we observe a crossover between the elastic and the plastic creep regimes; with *in situ* hydrostatic pressure only affecting the plastic regime. The effects of pressure reveal that, if engineered control of J_c can be achieved, the performance of coated conductors can be significantly improved in a range of fields and temperatures relevant for applications such as transformers, motors, and fault current limiters.

Acknowledgments

ORCID iDs

Lina Sang ⓘ https://orcid.org/0000-0002-6663-1265

References

[1] Fang L, Jia Y, Schlueter J, Kayani A, Xiao Z, Claus H, Welp U, Koshelev A, Crabtree G and Kwok W-K 2011 *Phys. Rev. B* **84** 140504
[2] Prozorov R, Kończykowski M, Tanatar M A, Thaler A, Bud'ko S L, Canfield P C, Mishra V and Hirschfeld P 2014 *Phys. Rev. X* **4** 041032
[3] Nakajima Y, Tsuchiya Y, Taen T, Tamegai T, Okayasu S and Sasase M 2009 *Phys. Rev. B* **80** 012510
[4] MacManus-Driscoll J, Foltyn S, Jia Q, Wang H, Serquis A, Civale L, Maiorov B, Hawley M, Maley M and Peterson D 2004 *Nat. Mater.* **3** 439
[5] Miura M, Maiorov B, Balakirev F F, Kato T, Sato M, Takagi Y, Izumi T and Civale L 2016 *Sci. Rep.* **6** 20436
[6] Cai C, Holzapfel B, Hänisch J, Fernandez L and Schultz L 2004 *Phys. Rev. B* **69** 104531
[7] Shabbir B, Wang X, Ghorbani S R, Shekhar C, Dou S and Srivastava O 2015 *Sci. Rep.* **5** 8213
[8] Sang L, Shabbir B, Maheshwari P, Qiu W, Ma Z, Dou S, Cai C, Awana V and Wang X 2018 *Supercond. Sci. Technol.* **31** 025009
[9] Kuklja M M and Kunz A B 1999 *J. Appl. Phys.* **86** 4428
[10] Londos C, Potsidi M, Bak-Misiuk J, Misiuk A and Emtsev V 2003 *Cryst. Res. Technol.* **38** 1058
[11] Misiuk A 2000 *Mater. Phys. Mech.* **1** 119
[12] Takahashi H, Igawa K, Arii K, Kamihara Y, Hirano M and Hosono H 2008 *Nature* **453** 376
[13] Alireza P L, Ko Y C, Gillett J, Petrone C M, Cole J M, Lonzarich G G and Sebastian S E 2008 *J. Phys.: Condens. Matter* **21** 012208
[14] Margadonna S, Takabayashi Y, Ohishi Y, Mizuguchi Y, Takano Y, Kagayama T, Nakagawa T, Takata M and Prassides K 2009 *Phys. Rev. B* **80** 064506
[15] Chen X, Lin H and Gong C 2000 *Phys. Rev. Lett.* **85** 2180
[16] Braithwaite D, Salce B, Lapertot G, Bourdarot F, Marin C, Aoki D and Hanfland M 2009 *J. Phys.: Condens. Matter* **21** 232202
[17] Tomita T, Schilling J, Chen L, Veal B and Claus H 2006 *Phys. Rev. Lett.* **96** 077001
[18] Tomita T, Schilling J, Chen L, Veal B and Claus H 2006 *Phys. Rev. B* **74** 064517
[19] Bud'ko S, Davis M, Wolfe J, Chu C and Hor P 1993 *Phys. Rev. B* **47** 2835
[20] Diederichs J, Reith W, Sundqvist B, Niska J, Easterling K E and Schilling J S 1991 *Supercond. Sci. Technol.* **4** S97
[21] Graser S, Hirschfeld P J, Kopp T, Gutser R, Andersen B M and Mannhart J 2010 *Nat. Phys.* **6** 609
[22] Alireza P, Zhang G, Guo W, Porras J, Loew T, Hsu Y-T, Lonzarich G, Le Tacon M, Keimer B and Sebastian S E 2017 *Phys. Rev. B* **95** 100505
[23] Sang L, Lu Y, Zhang Y, Zhong M, Zhu H, Liu Z, Guo Y, Gu Z, Qiu W and Fan F 2014 *Supercond. Sci. Technol.* **27** 065016
[24] Obradors X and Puig T 2014 *Supercond. Sci. Technol.* **27** 044003
[25] Shabbir B, Wang X, Ma Y, Dou S, Yan S-S and Mei L-M 2016 *Sci. Rep.* **6** 23044
[26] Bean C P 1964 *Rev. Mod. Phys.* **36** 31
[27] Gurevich A, Rzchowski M, Daniels G, Patnaik S, Hinaus B, Carillo F, Tafuri F and Larbalestier D 2002 *Phys. Rev. Lett.* **88** 097001
[28] Diaz A, Mechin L, Berghuis P and Evetts J 1998 *Phys. Rev. Lett.* **80** 3855
[29] Holesinger T G, Civale L, Maiorov B, Feldmann D M, Coulter J Y, Miller D J, Maroni V A, Chen Z, Larbalestier D C and Feenstra R 2008 *Adv. Mater.* **20** 391
[30] Gurevich A and Pashitskii E 1998 *Phys. Rev. B* **57** 13878
[31] Li X, Shi X, Wang J, Zhang Y, Zhuang J, Yuan F and Shi Z 2015 *J. Alloy. Comp.* **644** 523
[32] Higuchi T, Yoo S and Murakami M 1999 *Phys. Rev. B* **59** 1514
[33] Klein L, Yacoby E, Yeshurun Y, Erb A, Müller-Vogt G, Breit V and Wühl H 1994 *Phys. Rev. B* **49** 4403
[34] Civale L, Marwick A, McElfresh M, Worthington T, Malozemoff A, Holtzberg F, Thompson J and Kirk M 1990 *Phys. Rev. Lett.* **65** 1164
[35] Yeshurun Y, Malozemoff A and Shaulov A 1996 *Rev. Mod. Phys.* **68** 911
[36] Maiorov B, Baily S, Zhou H, Ugurlu O, Kennison J, Dowden P, Holesinger T, Foltyn S and Civale L 2009 *Nat. Mater.* **8** 398

[37] Gutierrez J, Llordes A, Gazquez J, Gibert M, Roma N, Ricart S, Pomar A, Sandiumenge F, Mestres N and Puig T 2007 *Nat. Mater.* **6** 367

[38] Llordes A, Palau A, Gázquez J, Coll M, Vlad R, Pomar A, Arbiol J, Guzman R, Ye S and Rouco V 2012 *Nat. Mater.* **11** 329

[39] Sun Y, Pyon S, Tamegai T, Kobayashi R, Watashige T, Kasahara S, Matsuda Y and Shibauchi T 2015 *Phys. Rev.* B **92** 144509

[40] Polat Ö, Sinclair J, Zuev Y L, Thompson J R, Christen D K, Cook S W, Kumar D, Chen Y and Selvamanickam V 2011 *Phys. Rev.* B **84** 024519

[41] Abulafia Y, Shaulov A, Wolfus Y, Prozorov R, Burlachkov L, Yeshurun Y, Majer D, Zeldov E, Wühl H and Geshkenbein V 1996 *Phys. Rev. Lett.* **77** 1596

[42] Taen T, Nakajima Y, Tamegai T and Kitamura H 2012 *Phys. Rev.* B **86** 094527